Fermi National Accelerator Laboratory

FERMILAB-Conf-90/84

The Optics of Secondary Polarized Proton Beams*

David C. Carey
Fermi National Accelerator Laboratory
P.O. Box 500
Batavia, Illinois 60510

May 1990

* Presented at the 3rd International Conference on Charged Particle Optics, Toulouse, France, April 24-27, 1990.

The Optics of Secondary Polarized Proton Beams

David C. Carey

Fermi National Accelerator Laboratory

Batavia, Illinois 60510 U.S.A.

Introduction

Polarized protons can be produced by the parity-violating decay of either Lambda or Sigma hyperons. A secondary beam of polarized protons can then be produced without the difficult procedure of accelerating polarized protons. The preservation of the polarization while the protons are being transmitted to a final focus places stringent limitations on the optics of the beam line.

The equations of motion of a polarized particle in a magnetic field have been solved to first order for quadrupole and dipole magnets. The lowest order terms indicate that the polarization vector will be restored to its original direction upon passage through a magnetic system if the momentum vector is unaltered. Higher-order terms may be derived by an expansion in commutators of the rotation matrix and its longitudinal derivative. The higher-order polarization rotation terms then arise from the non-commutivity of the rotation matrices by large angles in three-dimensional space.

In a secondary beam line, it is desirable to keep the higher-order terms as small as possible to preserve the polarization. However, a sequence of bending magnets known as a Siberian

snake can rotate the polarization vector by a large angle while leaving the momentum vector unchanged. In this case the higher-order terms provide the entire effect of the system, while the first-order terms sum to zero.

A polarized proton beam produced by decaying Lambda hyperons has been built and successfully operated in the Fermilab meson area. The polarization is determined by a correlation with the position of the proton in the phase space as projected back to the beginning of the beam line. This projected proton position is determined by hodoscopes at an intermediate focus. The polarization is destroyed at the intermediate focus, but restored at a final focus where the experimental target is located. The polarization produced by this method is transverse, but may be converted to longitudinal by a sequence of bending magnets located after the last focusing element, but before the experimental target.

Polarized protons from Sigma hyperons may be produced by a slight modification in the beam line. The first few meters of the beam line are transformed into a magnetic channel where momentum selection is done on the hyperons. The decay time of Sigma particles is about one third that of the Lambda particles, requiring that the magnetic channel be very short and that the field be quite strong. The remainder of the magnetic channel is the same as that for Lambdas and does momentum selection on the polarized protons. The combination of momentum selections means that only protons resulting from backward decays in the center of mass are transmitted. No hodoscopes are needed as the entire beam is longitudinally polarized. The flux is comparable to that for the polarized part of the Lambda produced beam

Equation of Motion

The classical equation of motion of the spin vector s, of a particle of charge e, mass m, and ratio g of magnetic moment to classical moment is

$$\frac{\mathbf{ds}}{\mathrm{dt}} = \mathrm{g}\ \frac{\mathrm{e}}{2\mathrm{m}}\ \mathbf{s} \times \mathbf{B} \tag{1}$$

A relativistic generalization of this equation was first derived by Bargmann, Michel, and Telegdi.[1] A complete derivation can be found in reference 2. The derivation consists basically of expressing both sides of equation (1) as tensors and matching coefficients. The polarization vector is expressed in the center of mass of the proton so that its direction is not simply dominated by the velocity of the particle. The magnetic field is expressed in the laboratory. The resulting equation for the polarization vector of a particle moving in a magnetic field is then:

$$\frac{\mathbf{dP}}{\mathrm{dt}} = \frac{\mathrm{e}}{\mathrm{m}\gamma}\ \mathbf{P} \times \left[\frac{\mathrm{g}}{2}\ \mathbf{B}_{\mathrm{L}} + (1 + \frac{\mathrm{g}-2}{2}\ \gamma)\mathbf{B}_{\mathrm{T}}\right] \tag{2}$$

Here the magnetic field is separated into longitudinal and transverse components, indicated by appropriate subscripts. This arises because the magnetic field and the polarization vector are expressed in different coordinate systems.

If the magnetic moment were equal to the Dirac moment, so that g exactly equalled two, the expression inside the brackets would reduce to **B**. The precession equation for a particle

in motion would be the same as that of a particle at rest, save for the use of proper time in the derivative. The anomalous part, however, contains a factor γ, so that, relative to the Dirac part, it increases in importance as the kinetic energy increases. For protons the anomalous part of the magnetic moment is greater than the Dirac part, even at rest. As the energy is increased and the anomalous part becomes increasingly greater, the factors of γ cancel, and the rate of polarization precession is independent of energy. For a highly relativistic proton, a rotation of 90^o is produced by a field integral of 27.4 kG-m.

The two parts of the magnetic field $\mathbf{B}_L$ and $\mathbf{B}_T$ are respectively longitudinal and transverse with respect to the direction of the individual trajectory. In the usual beam line coordinate system, the components of $\mathbf{B}_T$ are given by

$$B_{Tx} = \frac{(1+hx)^2+y'^2}{T'^2}\,B_x - \frac{x'y'}{T'^2}\,B_y - \frac{(1+hx)x'}{T'^2}\,B_s \tag{3}$$

$$B_{Ty} = -\frac{x'y'}{T'^2}\,B_x + \frac{(1+hx)^2+x'^2}{T'^2}\,B_y - \frac{(1+hx)y'}{T'^2}\,B_s$$

$$B_{Tz} = -\frac{(1+hx)x'}{T'^2}\,B_x - \frac{(1+hx)y'}{T'^2}\,B_y + \frac{x'^2+y'2}{T'^2}\,B_s$$

where h is the local curvature and

$$T'^2 = (1+hx)^2 + x'^2 + y'^2 \tag{4}$$

In solving equation (2), four different approximations are made. The first two are sim-

plifications of the equation of motion, and the second two are the expansion by orders in the expression of the solution. The latter two will be described in the next section.

The first approximation in simplifying the equation of motion at high energies is to consider only the B_T term in the brackets, since it is favored by a factor of γ. The second is to take the components of B_T along the particular orbit as being those along the reference orbit. We are then keeping only those terms of the lowest order in x' and y' in equation (3).

For a particular trajectory, we may define a polarization transfer matrix M, so that the polarization is given in terms of its initial value by

$$\mathbf{P} = M\mathbf{P}_o \tag{5}$$

An orthogonal transformation can be written as the exponential of an antisymmetric matrix, so that M takes the form

$$M = e^H \tag{6}$$

The magnetic field can be incorporated into an antisymmetric matrix F, so that F and H become

$$F = \begin{bmatrix} 0 & 0 & -B_y \\ 0 & 0 & B_x \\ B_y & -B_x & 0 \end{bmatrix} \qquad H = \begin{bmatrix} 0 & 0 & -\theta_y \\ 0 & 0 & \theta_x \\ \theta_y & -\theta_x & 0 \end{bmatrix} \tag{7}$$

Dividing equation (1) by βc to express the motion as a function of distance along the reference orbit, we derive

$$\frac{d}{dz}\, e^{H} = \frac{e}{p}\,(1+\frac{g-2}{2}\,\gamma)Fe^{H} \tag{8}$$

The matrix H is the dual of a rotation vector θ, just as F is the matrix dual of the magnetic field B. The matrix M has the form

$$M = \begin{bmatrix} n_x^2 + n_y^2 C & n_x n_y (1-C) & -n_y S \\ n_x n_y (1-C) & n_x^2 C + n_y^2 & n_x S \\ n_y S & -n_x S & C \end{bmatrix} \tag{9}$$

$$\theta_x = n_x \theta_p \qquad \theta_y = n_y \theta_p \qquad \theta_p = \sqrt{\theta_x^2 + \theta_y^2}$$

$$S = sin\theta_p \qquad C = cos\theta_p$$

Solution of the Equation of Motion

Since H is a matrix, we must expand the left side of equation (3) as a series of commutators. Truncating the series after the first four terms yields

$$\frac{d}{dz}\, e^{H} = \frac{dH}{dz}\, e^{H} + \frac{1}{2}\,[H, \frac{dH}{dz}]\, e^{H} + \frac{1}{6}\,[H,[H, \frac{dH}{dz}]]e^{H} + \frac{1}{24}\,[H,[H,[H, \frac{dH}{dz}]]]e^{H} \tag{10}$$

Equation (10) is then substituted into equation (8) and all terms save the first are transferred to the right. The equation can then be solved by successive approximation. Including only the first two terms, we derive

$$H = \frac{e}{p}\,(1+\frac{g-2}{2}\,\gamma)\ \int_0^\ell \mathrm{F dz} - \frac{1}{2}\frac{e^2}{p^2}\,(1+\frac{g-2}{2}\,\gamma)^2\ \int_0^\ell \int_0^z\,[\mathrm{F}(\zeta),\mathrm{F(z)}]\mathrm{d}\zeta\mathrm{dz} \qquad (11)$$

The first term gives the lowest-order solution to the differential equation, as if the magnetic fields were all pointing in the same direction. Taking this term alone is the first of the two approximations to be made in the solution of the equation of motion. Expressed in terms of components, the lowest-order solution for the rotation angles is

$$\theta_x = \frac{e}{p}\,(1+\frac{g-2}{2}\,\gamma)\int_0^\ell \mathrm{B_x dz} \qquad (12)$$

$$\theta_y = \frac{e}{p}\,(1+\frac{g-2}{2}\,\gamma)\int_0^\ell \mathrm{B_y dz}$$

The lowest-order equations of motion for the trajectory coordinates themselves are

$$x'' + \frac{e}{p}\,\mathrm{B_y} = 0 \qquad (13)$$

$$y'' - \frac{e}{p}\,\mathrm{B_x} = 0$$

These two equations contain some higher-order contributions. The momentum p is that of a general trajectory, and the expansion of the field may contain higher-order terms. Integrating these equations over the length of the beam line yields

$$x'_f - x'_i = -\frac{e}{p}\int_0^\ell B_y dz \tag{14}$$

$$y'_f - y'_i = \frac{e}{p}\int_0^\ell B_x dz$$

Comparing these equations to those for θ_x and θ_y, we derive

$$\theta_x = (1+\frac{g-2}{2}\gamma)(y'_f - y'_i) \tag{15}$$

$$\theta_y = -(1+\frac{g-2}{2}\gamma)(x'_f - x'_i)$$

For the net polarization rotation to be zero to lowest order, the initial and final trajectory directions must be the same. If the beam line also produces a point-to-point focus, then the net transformation in both planes must be the identity. Generally, an identity transform can be achieved for only a single momentum. Considering the first-order trajectory alone is the second of the two approximations in the solution of the equations of motion.

The second term of equation (11) involves the integral of a commutator over a triangular domain. The matrix obtained from the commutator is the dual of a vector formed from the cross product of the magnetic field vectors B at two different longitudinal locations. Such a term represents a rotation about the longitudinal axis, which, however, can be large, since it

is produced by the transverse field and its coefficient contains the factor γ. It is because of this and other similar higher-order terms that snakes can rotate or reverse the polarization.

If the first-order approximation to the polarization transfer matrix is evaluated for each magnetic element and the results multiplied together, then the result will contain that portion of the commutator where the two longitudinal locations are in different elements. It will still not contain the contribution from a single element, for example, what might be called the "self-snaking" term for a quadrupole. It may be useful to examine the double and multiple integrals of commutators for a lattice as well as the lowest order field integral for a periodic structure to maximize the degree of polarization preservation.

Production of Polarized Protons from Λ Hyperons

The polarized protons used in the new beam line at Fermilab are produced in the parity-nonconserving decays of Λ particles. The layout of the beam line is illustrated in Fig. 1. The incoming 800-GeV/c primary-proton beam strikes a beryllium target and creates unpolarized lambdas. The intensity of Λ hyperons can be maximized by centering the beam-line acceptance at 0° production angle. In the unpolarized Λ rest frame, the decay $\Lambda \rightarrow p + \pi^-$ occurs isotropically and the decay-proton polarization is 64% with the spin direction along the proton momentum.

In the laboratory reference frame, the trajectories of the protons from the Λ decays can be traced back to the plane of the production target. Protons with components of their momentum transverse to the Λ direction appear to come from a virtual source displaced

from the actual Λ source, as shown in Fig. 2. For a fixed Λ decay distance, protons with the same decay angle project back to the same point on the virtual source, regardless of the direction of the Λ trajectory. The transverse spin component of the proton is then correlated to its projected position at the virtual source.

Obtaining good separation of the polarization states at the virtual source involves two requirements. First, the size of the real production target must be very small compared to the size of the virtual source. This requirement provides adequate resolution for identification of the proton polarization state. The beryllium production target has a width of 1.5 mm, height of 5mm, and length of 30 cm (0.74 interaction length). The target length is limited by both the divergence of the primary proton beam and the angular acceptance of the secondary beam, and also by the accuracy of the target alignment. The virtual source size extends to approximately 1 cm on each side of the target.

Second, the distance at which the Λ decays from the target must be reasonably well defined. At the production target, two dipole magnets eliminate unwanted charged particles from the beam, as shown is Fig. 1. Noninteracting primary-beam protons are deflected downward into a beam dump. Charged particles produced at the target are bent away from the channel acceptance and into a brass absorber. Also, the charged particles from Λ decays occurring too close to the production target are swept from the beam. Only those Λ decays occurring between 9 and 30 m from the production target are accepted. The virtual source displacement of such decays is larger than that of decays near the production target, allowing a more precise determination of the polarization direction. Approximately one-half of the

lambdas decay in this region. Remaining neutral particles consist mainly of neutrons and gamma rays. They proceed to a neutral beam dump while the positively-charged particles from Λ and K^0 decays are bent downward, below the dump.

Polarized-Proton Beam Description

The bending and focusing operations of the beam-transport system are decoupled as completely as possible from each other. The bending magnets occur in achromatic sets of four, entirely contained between two quadrupole doublets. Any displacement or angular deflection due to a bend in the beam is restored by three subsequent bends. Each set of four bending dipoles produces no net momentum dispersion or particle spin precession. Two effects from the dipole magnets, edge focusing and magnetic-field nonuniformities, could possibly distort the image from quadrupole focusing. Both of these effects are small for this beam line.

There are two sets of four bending magnets in the beam line, as shown in Fig. 1. The first set bends the protons around the neutral dump area. The second set, located at the intermediate focus, is used for the beam-momentum measurement. Two quadrupole doublets bring the beam to a focus at an intermediate location downstream of the production target and virtual source. Two more doublets provide a final focus. The intermediate focus is situated halfway between the source and the experimental target, 160 m downstream of the primary target. Sets of hodoscopes at the intermediate focus determine both the trajectory momentum and the projected proton initial transverse position. The final focus is located at the experimental target position, which is 320 m downstream of the production target.

The actual position of the intermediate focus along the beam line depends on the momentum of the beam particles. Higher-momentum particles focus farther downstream of the nominal-momentum focal position, while lower-mmomentum particles focus farther upstream. The momentum measurement from the beam-tagging hodoscopes is used to provide an improved polarization determination.

The neutral beam dump region is located approximately 70 m from the production target and 50 m from the primary beam dump. The charged particles are partially momentum selected at this bend to approximately $\pm$ 30 % of the 185-Gev/c beam-momentum value. The neutral beam dump is embedded inside the apertures of six large beam-transport magnets.

An adjustable, vertical collimator, located upstream of the intermediate focus position, can be used to vary the beam-particle momentum bandpass. This collimator has a maximum aperture height of 12.7 cm. At an aperture height of 3.2 cm, a $\pm$ 9% momentum bite about the nominal momentum value of 185 GeV/c is mostly transmitted. Significant tails of about 3% in the momentum distribution occur because the collimator is not situated at the intermediate focus.

The beam-particle polarization is determined from the correlation between the position of the virtual source and the proton momentum direction, which, in turn, is correlated to the proton polarization direction. This correlation is displayed in Fig. 2, where the average final particle polarization is plotted as a function of the horizontal position at the intermediate focus. At the intermediate beam focal point, each beam particle within the acceptance is tagged to determine its momentum and polarization. The particle tagging measures only the

horizontal component of the transverse proton polarization. Using this method, it is possible to use protons with both signs of this horizontal component simultaneously. The pion coming from the Λ decay is not tagged or otherwise used to obtain the proton polarization.

The requirements of preserving the proton polarization are most easily satisfied by constructing the beam line from two telescopic systems placed back-to-back. For each half of the beam line the two conditions of point-to-point focusing and parallel-to-parallel focusing are imposed in each plane. The second half of the beam line is just the longitudinal reversal of the first half. This configuration preserves the correlation between the final polarization state and the intermediate image of the virtual-source position. The mirror symmetry has the effect of minimizing the contribution of the commutator term in equation (11).

The entire beam line then consists of four quadrupole-magnet doublets producing a first-order identity transfer matrix. For either of the two sets of four dipole magnets bending the beam, the ray transform is that of a drift space and the polarization transform is an identity matrix. An identity transform in beam focusing gives spin transparency, or no net spin precession.

Computer programs were used to design and evaluate the performance of the beam. The program TRANSPORT[3] was used to determine the drift lengths and the quadrupole and dipole-magnet strengths that satisfied the constraints on the beam optics and the polarization. The beam-transport program TURTLE[4] was used to understand detailed beam properties. Included in the simulations were chromatic effects, finite-size source effects, and magnetic field aberrations.

Several extensions to the existing computer programs were added to simulate the beam line in greater detail. For example, the precession of the particle spin through quadrupole magnets was incorporated. The beam rates and backgrounds used in the Monte Carlo simulation of the beam line were calculated from data gathered in previous experiments, such as the Λ, K^0, and π^o production cross sections.

Two threshold Cerenkov counters, each 21.4 m long and using helium gas at a pressure of 0.3 atm, are used to separate the polarized protons from the pion contamination coming from K^0 decays. The Cerenkov counters are set to reject pions with maximum efficiency and veto only a few protons. Each counter measured a 13% pion contamination in the polarized proton beam.

Spin-Rotation Magnets

A spin-precession rotator, loosely called a "snake", consists of a set of magnets that change the beam-particle polarization state from one direction to another. No overall perturbation of the beam-particle trajectory is allowed; the bends and displacements of the trajectory must cancel while traversing the snake magnets. A spin rotator is used in the beam line for two reasons: (1) to periodically reverse the polarization direction so that experimental systematic errors are controlled, and (2) to change the spin direction from horizontal (S spin direction), which is the spin component actually tagged, to vertical (N spin direction) or longitudinal (L spin direction) for different experimental measurements. The operation of the snake is based on the noncommutativity of rotations in orthogonal directions and the fact that the polarization rotation angles are much larger than the trajectory bend

angles. The sum of the bends in the beam-particle trajectory from the set of magnets is zero. The sum of noncommutative rotations describing the particle spin precession through the snake is large.

The magnetic fields of the snake magnets are transverse to the beam direction. The advantage of using magnetic fields directed in this manner is that for a given spin precession angle, the magnetic field value remains nearly independent of the particle momentum at high energies. For snakes with magnetic fields aligned along the beam axis, the magnetic field must increase with the growing momentum for a given spin-precession angle. Solenoids, for example, become impractical at high beam-momentum values.

The Fermilab MP beam-line spin-rotation ("MP snake") system consists of 12 dipole magnets, each of which precesses the particle spin by 45° A snake magnet is 99.1 cm long, and has a 1.38 T magnetic field. The magnet pole faces are tilted 45° with respect to the vertical axis.

The system can be switched electrically to give either a Type I or a Type II snake configuration. A type I snake system has an overall rotation around the beam axis with the polarization direction changed from horizontal to vertical (S $\rightarrow$ N). Eight magnets are used from the 12 total magnets, with numbers 1, 2, 4, and 11 not being used.

A Type II snake system has an overall rotation about the vertical axis with the polarization direction changed from horizontal to longitudinal (S $\rightarrow$ L). All 12 magnets are used in this transformation; each of four groups containing two dipole magnets gives a 90° spin

precession, and each of the four remaining dipole magnets provides a 45° spin precession. Both configurations are described in greater detail in Ref. 5.

Polarized-Beam Performance

The polarized beam is monitored by several scintillation counter hodoscopes, which are shown in Fig. 1. Two sets of three hodoscopes each measure particle trajectories in the horizontal and vertical directions at the intermediate focus. Other sets of horizontal and vertical hodoscopes are located just upstream and downstream of the snake magnets, and measure the particle trajectories entering the experimental target region. By using these beam hodoscopes, the properties of the beam line can be studies in detail.

By the use of this extensive beam-line instrumentation, many properties of the polarized beam can be measured directly, such as the beam profile, phase space, and spatial and angular magnification. The beam size at the intermediate focus agrees with the expected size to within 5%. By projecting the measured particle trajectories at different locations along the beam line in the intermediate-focus and final-focus regions, the foci were found at the expected positions with no distortion of the beam. The beam acceptance is determined principally by the collimator within the charged-particle sweeping magnets located at the production target.

The elliptical phase-space area as measured at the intermediate focus is 12 mm-mrad for xx' and 9 mm-mrad for yy'. Comparing the horizontal and vertical positions of a given trajectory at the intermediate focus with those at the final focus provides information on

the spatial magnification of the beam. The spatial magnification in the horizontal direction is about 0.9, with an inverted image at the intermediate focus. The angular magnification is about -1.1 in the horizontal direction. Both the measured emittance and magnifications corroborate the predictions of beam-transport calculations.

The total number of protons with a ±9% momentum bite and collimator aperture of 3.2 cm that reach the experimental target is $9 \cdot 10^6$ when 10^{12} protons per 20-sec spill are incident on the 0.74 interaction length production target. Roughly half the protons have a polarization magnitude greater than 35%. The total number of tagged protons is $6 \cdot 10^6$ and the number of these with a polarization magnitude greater than 35% is $3 \cdot 10^6$. The tagged intensities are less than the total intensity because of detector and electronics limitations. The systematic error on all intensities is estimated to be ±20%, arising primarily from the uncertainty in the primary proton beam intensity.

Polarized antiproton beam properties were also studied, but the amount of data is limited. The total number of antiprotons at the experimental target is $5 \cdot 10^5$, with 10^{12} incident protons per 20-sec spill on the production target and a ±9% momentum bite. This rate is 18 times lower than that for polarized protons. The number of background pions is about 5 times the total number of polarized antiprotons. Despite the snall amount of data, thc method of beam tagging was shown to work for antiprotons.

Polarized Protons from Σ^+ Hyperons

The decay of a Σ^+ hyperon also yields a proton whose polarization is correlated with

its momentum in the hyperon center of mass. The positive charge of the hyperon allows momentum selection both on it and on the proton. A beam of longitudinally polarized protons can be produced by backward decays in the center of mass. The Λ hyperon being neutral, does not allow momentum selection.

The use of Σ^+ hyperons to produce polarized protons was first suggested by Rafil Rzaev, a visitor to Fermilab from Serpukhov. He was primarily concerned with the existing 200 GeV polarized beam in the Fermilab meson area. Since then interest has been shown in polarized protons by other experimental collaborations. These experiments are at the ends of beam lines in existing tunnels. These tunnels are curved and are well suited to a Σ^+ produced polarized proton beam which has a net bend.

The targetting scheme for Σ^+ is illustrated in figure 3. The magnets shown are set to bend 310 GeV Σ^+ by 12 mr onto the axis of the polarized proton beam. The 800 GeV incident protons are deflected only 4.2 mr toward a beam dump.

The polarized proton beam is tuned to a momentum of 200 GeV/c and is unchanged from its use with Λ hyperons. The protons resulting from the Σ^+ decay have a momentum which ranges from 65 to 96 percent of the Σ^+ momentum. By setting the proton momentum to the lower end of this range, we select only backward decays in the center of mass. No particles of any momentum, directly produced at the target can reach the end of the polarized proton channel.

The masses of the two hyperons, Λ and Σ^+, are comparable but the Σ^+ decays about

three times as rapidly as the Λ. At 310 GeV the decay length of the Σ^+ is 6.3 meters, while that of the Λ is 22 meters. Essentially all protons are produced before the Σ^+ particles reach the first quadrupole.

The branching ratio of Λ into protons is higher than that of Σ^+ into protons by a factor which is no larger than are the uncertainties in flux estimates. The correlation of polarization with decay direction for a Σ^+ hyperon is 98%. For a Λ hyperon it is only 65%.

In the Σ^+ produced beam, the average polarization was calculated to be 63 percent. The flux is approximately 10 percent of the proton flux for the Λ produced beam. However, in the Λ produced beam, a polarization of 35% or greater is achieved for only about 50% of the tagged flux. In addition, the average polarization is greater for the Σ^+ produced beam. The quantity that is statistically significant in the experimental analysis is the square of the polarization times the beam intensity. For the Σ^+ beam this figure of merit is then close to that of the Λ produced beam The Σ^+ production was estimated by combining measured ratios of Σ^+ to π^+ at 400 GeV with scaled π^+ production rates at 200 GeV. The production rates of the Σ^+ and Λ appear to be equal to the accuracy that flux estimates can be made. A variety of background processes produce other particles. The production of muons from π^+ is comparable to that of protons from Σ^+. Among produced hadronic particles the process $\Sigma^+ \rightarrow \pi^+$ provides roughly a 4% background.

The use of the Siberian snake at the end of the beam line allows the transformation of any direction of polarization into any other direction. The two transverse polarization modes can then be alternated by reversing the fields of the snake magnets. Any systematic effects

associated with asymmetric beam line acceptances will thereby be reduced.

References

1. V. Bargmann, L. Michel, and V. L. Telegdi, Phys. Rev. Letters 2, 435 (1959).

2. D. C. Carey, *The Optics of Charged Particle Beams*, Harwood Academic Publishers, New York, 1987.

3. K. L. Brown, F. Rothacker, D. C. Carey, and Ch. Iselin, TRANSPORT, A Computer Program for Designing Charged Particle Beam Transport Systems, SLAC Report No. 91 (1977).

4. D. C. Carey, K. L. Brown, and Ch. Iselin, DECAY TURTLE, A Computer Program for Simulating Charged Particle Beam Transport Systems, Incuding Decay Calculations, SLAC Report No. 246 (1982).

5. D. G. Underwood, "A Survey of Eight-Magnet Spin Precession Snakes", Nuclear Instruments and Methods 173, 351 (1980).

Figure Captions

1. The layout of the Fermilab polarized proton beam. The polarized protons are produced by the parity-violating decay of Lambda hyperons and are subsequently transmitted without net polarization precession to the experimental target.

2. The relationship between the polarization direction and the virtual source location. The proton polarization is correlated with its momentum in the Lambda center of mass. The proton momentum in the laboratory, when projected back to the target plane, gives a virtual source position transversely displaced from the actual source position for the hyperons.

3. The targetting scheme for the Sigma hyperons. Because the Sigma particles are charged, a magnetic channel can perform momentum selection. The subsequent channel for the protons from the decaying Sigmas is identical to that used for the Lambda beam. The proton channel is set for a lower momentum than the Sigma channel, selecting only protons produced by backward decays in the Sigma center of mass. The center-of-mass decay direction is then correlated with the proton polarization.

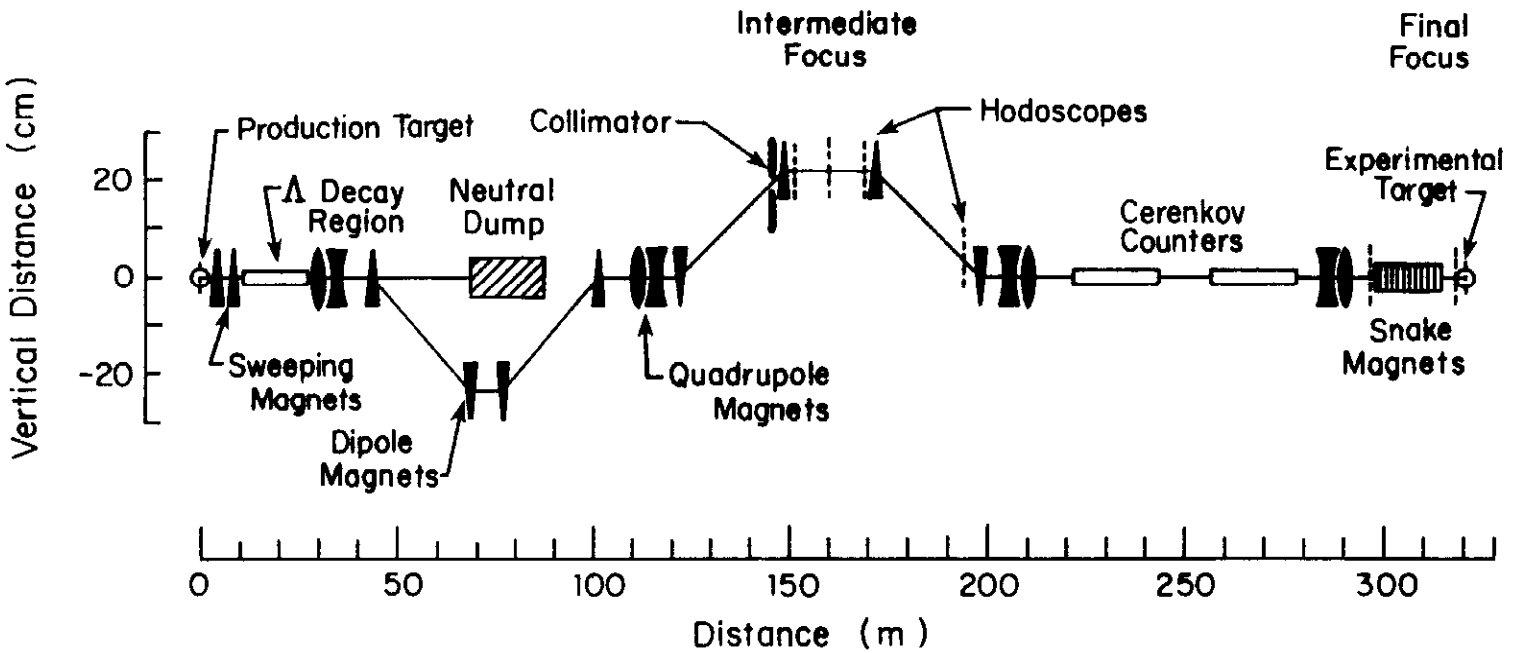
Intermediate
Focus
Final
Focus
Production Target
Collimator
Hodoscopes
Experimental
Target
Λ Decay
Region
Neutral
Dump
Cerenkov
Counters
Vertical Distance (cm)
20
0
-20
Sweeping
Magnets
Quadrupole
Magnets
Snake
Magnets
Dipole
Magnets
0
50
100
150
200
250
300
Distance (m)

Figure 1

Figure 2

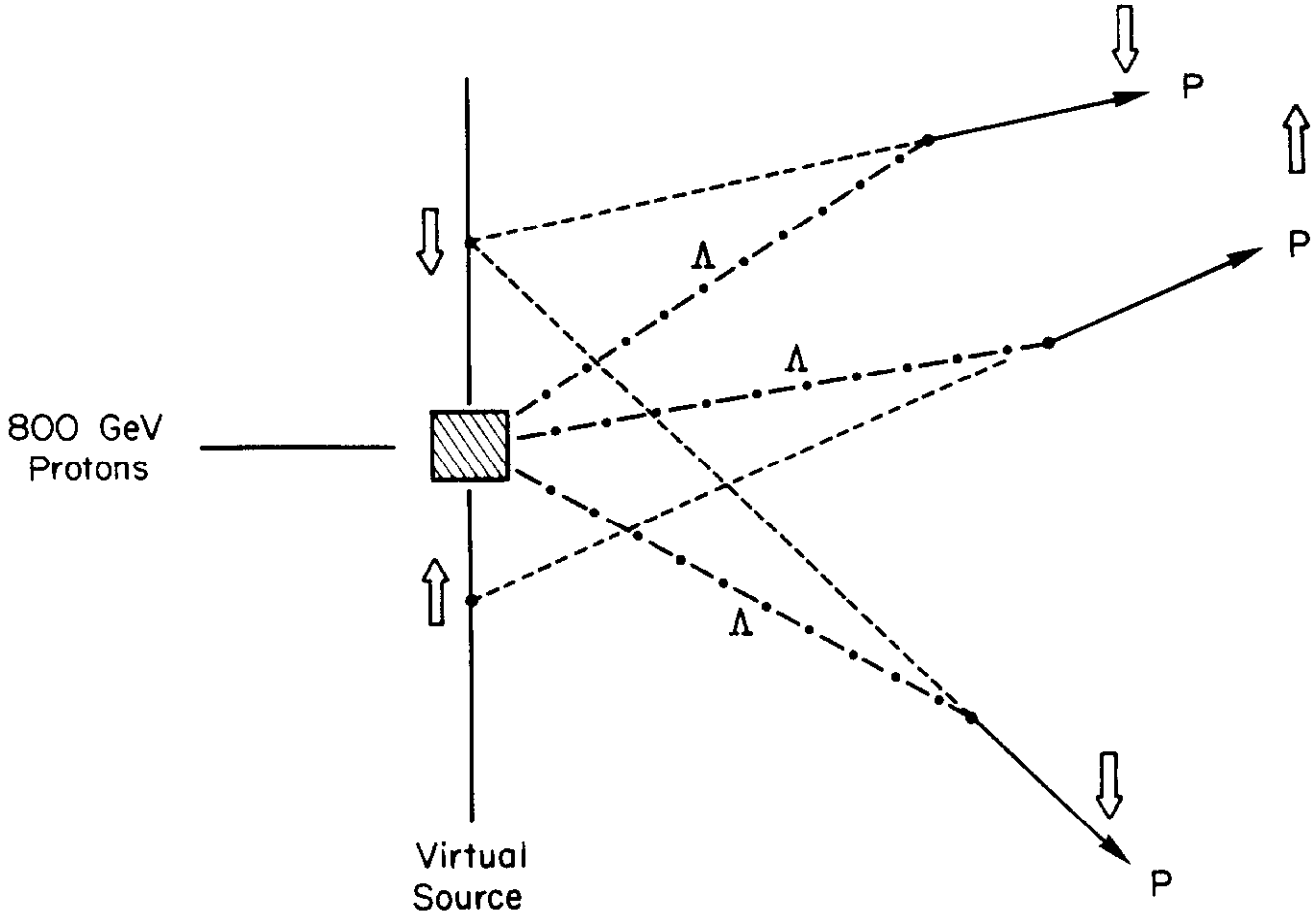

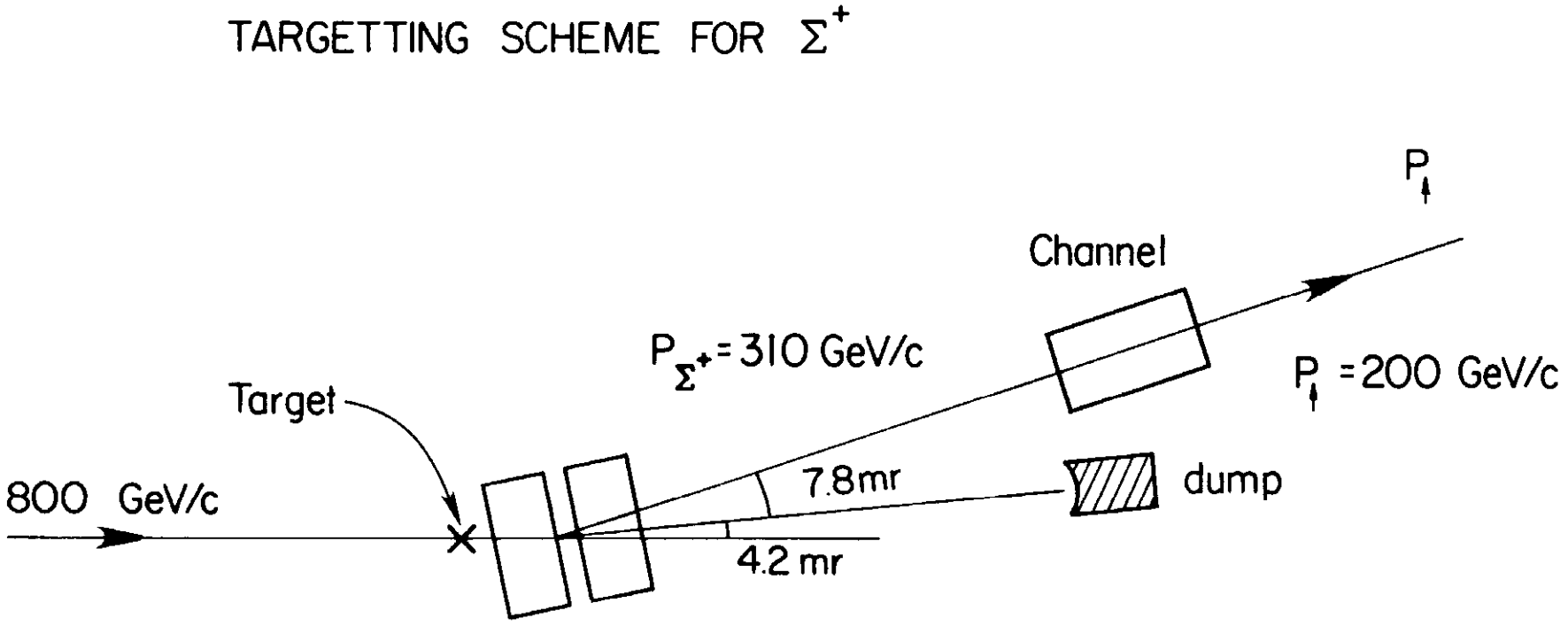
TARGETTING SCHEME FOR Σ^+
$P_\uparrow$
Channel
P_{Σ^+} = 310 GeV/c
$P_\uparrow$ = 200 GeV/c
Target
800 GeV/c
7.8mr
dump
4.2 mr

Figure 3